Copyright Warning & Restrictions

The copyright law of the United States (Title 17, United States Code) governs the making of photocopies or other reproductions of copyrighted material.

Under certain conditions specified in the law, libraries and archives are authorized to furnish a photocopy or other reproduction. One of these specified conditions is that the photocopy or reproduction is not to be "used for any purpose other than private study, scholarship, or research." If a, user makes a request for, or later uses, a photocopy or reproduction for purposes in excess of "fair use" that user may be liable for copyright infringement,

This institution reserves the right to refuse to accept a copying order if, in its judgment, fulfillment of the order would involve violation of copyright law.

Please Note: The author retains the copyright while the New Jersey Institute of Technology reserves the right to distribute this thesis or dissertation

Printing note: If you do not wish to print this page, then select "Pages from: first page # to: last page #" on the print dialog screen

ABSTRACT

BRIGHT LIGHT THERAPY AND DEPRESSION: ASSESSING SUITABILITY USING ENTRAINMENT MAPS

by
Charles A. Mainwaring

Bright Light Therapy has been shown to be efficacious to mood disorders including Major Depression. Researchers use the Jewett-Forger-Kronauer model of the circadian rhythm with the Unified Model of melatonin including a mathematical term implementing feedback from the melatonin system into the circadian system to quantify the effects of bright light. Early investigations into intrinsic period, light sensitivity, and the circadian pacemaker's sensitivity to blood melatonin concentration may be indicators of subsets of patients with long intrinsic periods exhibiting symptoms of depression.

BRIGHT LIGHT THERAPY AND DEPRESSION: ASSESSING SUITABILITY USING ENTRAINMENT MAPS

by
Charles A. Mainwaring

A Thesis
Submitted to the Faculty of
New Jersey Institute of Technology
in Partial Fulfillment of the Requirements for the Degree of
Master of Applied Mathematics

Department of Mathematical Sciences

May 2023

APPROVAL PAGE

BRIGHT LIGHT THERAPY AND DEPRESSION: ASSESSING SUITABILITY USING ENTRAINMENT MAPS

Charles A. Mainwaring

Dr. Amitabha K. Bose, Thesis Co-Advisor — Date
Professor of Mathematical Sciences, NJIT

Dr. Casey O. Diekman, Thesis Co-Advisor — Date
Associate Professor of Mathematical Sciences, NJIT

Dr. Horacio G. Rotstein, Committee Member — Date
Professor of Biological Sciences, NJIT

BIOGRAPHICAL SKETCH

Author: Charles A. Mainwaring

Degree: Master of Science

Date: May 2023

Undergraduate and Graduate Education:

- Master of Science in Applied Mathematics,
  New Jersey Institute of Technology, Newark, NJ, 2023
- Bachelor of Arts, Self-Designed–Mathematics and Biochemistry
  Emerson College, Boston, MA, 2021
- Associate of Arts, Psychology
  Argosy University Online, Phoenix, AZ, 2015

Major: Applied Mathematics

Presentations:

Charles Mainwaring, "BRIGHT LIGHT THERAPY AND DEPRESSION: ASSESSING SUITABILITY USING ENTRAINMENT MAPS," *Math Bio Seminar*, NJIT, April 05, 2023.

Charles Mainwaring, "SSRIs v TCAs: Side Effects Approximation using Meta-analyses of Drop-out Odds-ratios" *Frontiers in Applied and Computational Mathematics (FACM)*, NJIT, May 20, 2022.

I dedicate my work to my parents for their endless love and support.

ACKNOWLEDGMENT

First and foremost, I would like to thank my Thesis Advisors Dr. Casey Diekman and Dr. Amitabha Bose for their kind, patient, and thorough guidance.

Thanks to the Thesis Committee for insightful discussion. Thanks to Dr. Horacio Rotstein for discussions related to dynamical systems and conditions for oscillatory behavior.

Thanks to NJIT and the Department of Mathematical Sciences for offering me admission.

Thanks to HPC for the much needed computational resources which allowed the thesis to be completed in a reasonable amount of time.

Thanks to the Math Bio group for listening to my thoughts and letting me present on the thesis.

Thanks to Soheil Saghafi for providing me with thesis resources and teaching me how to use the high-performance computing resources.

TABLE OF CONTENTS

LIST OF TABLES

Table **Page**

LIST OF FIGURES

LIST OF FIGURES
(Continued)

Figure **Page**

CHAPTER 1

INTRODUCTION

1.1 Background

Bright Light Therapy (BLT) involves having a patient sit in front of a light box emitting high intensity light for a sustained period. BLT has a history of demonstrated efficacy in a variety of mood disorders [9, 16]. In this thesis, we assess the potential efficacy of BLT on Major Depression. We believe they have illuminated some key mechanisms necessary to determine whether BLT would be helpful for the patient and to determine what time to administer bright light based on key parameters to maximize benefits.

Prior research has assessed the efficacy of BLT by assessing melatonin concentrations relative to Core Body Temperature (CBT) and entrainment maps of various combinations of intrinsic periods, light sensitivities, and feedback to the circadian system from the melatonin generating system.

At its core, this thesis is about circadian rhythms. Circadian rhythms are a set of periodic organic processes that serve to keep organs synchronized so as to promote a unified purpose. The circadian pacemaker serves as a master clock, coordinating the activity of the circadian rhythms in line with feedback from the environment. The circadian pacemaker is composed of the cells of the suprachiasmatic nucleus (SCN) [13]. Additionally, it keeps humans and other organisms attuned to 24-hour day. In part, the pacemaker is responsible for making people feel tired during bedtime. So, barring crises or deliberate interventions, one should not feel hyperactive just before going to sleep. The fact that this statement is true for most people day after day is a testament to the pacemaker's competence.

Entrainment refers to a phenomenon whereby multiple, coupled, oscillating systems come to match phase with one another [12, 15]. In this case, the circadian pacemaker entrains to the environment using cues. The environmental cues the circadian pacemaker uses are called 'zeitgebers' and the predominate zeitgeber is light. This means that using only light as an input to a model of the pacemaker provides an accurate enough representation of pacemaker activity for us to draw meaningful conclusions. When discussing entrainment in the thesis, we refer specifically to entrainment of the circadian pacemaker to 24 hours. Furthermore, the primary mathematical tool used to study entrainment is the Entrainment Map. Entrainment Maps in the context of circadian rhythms were introduced by Diekman and Bose [4–6].

There is strong evidence that the efficacy of BLT is based on the circadian pacemaker. Specifically, it's based on the fact that light is the most influential zeitgeber. Furthermore, increasing the intensity of light increases influence of light on the circadian pacemaker. For example, running a simulation of the model using pure dark input may yield a limit cycle for the system. However, there is no entrainment in that case. On the other hand, given a particular combination of parameter values, introducing a sufficient duration of light at a high enough intensity yields a limit cycle that does entrain.

The model is based on retinal protein concentration which is used up and recycled after contact with light. The proteins trigger neural stimulation resulting in signals to the SCN. The SCN sends an inhibitory signal to the pineal gland which generates melatonin. The intensity of the inhibition directly corresponds with the intensity of light.

1.2 Structure of the Thesis

Chapter 2 is dedicated to the mathematical model which is separately composed of three mathematical models devised separately by others. The composite models

are: the FJK model [7] [10]; the Unified Model of melatonin [1]; and the Exogenous Model of melatonin [2]. The latter model provides a component for feedback from the melatonin portion of the model to the circadian portion.

Chapter 3 considers entrainment maps to assess how various parameters effect properties of entrainment. These parameters include the intrinsic period of the the oscillators, their sensitivity to light as well as their ability to process melatonin. We then show how the the timing of bright light therapy affects the ability to entrain and the ensuing properties when this does occur.

Chapter 4 explores cases based on evidence that healthy individuals and depressed patients have different intrinsic periods [11]. We assigned particular combinations of τ_C, p, and $Mmax$ as depressed based on the time relationship between minimum core body temperature and maximum melatonin and assessed the effects of bright light administered at different hours [8].

CHAPTER 2

THE MATHEMATICAL MODEL

2.1 The Model

The model is an assemblage of parts of three related mathematical models. The model is composed of the following differential equations:

$$\frac{dC}{dt} = h(A + B - M[H_2]) \tag{2.1}$$

$$\frac{dA}{dt} = h\left(\mu\left(A - qA^3\right) - C\left((\frac{24}{0.99669\tau_C})^2 + kB\right) - M[H_2]\right) \tag{2.2}$$

$$\frac{dn}{dt} = \gamma(\alpha[I](1-n) - \beta n) \tag{2.3}$$

$$\frac{dH_1}{dt} = \frac{m[\Phi]r[I] - H_1}{\tau_{H_1}} \tag{2.4}$$

$$\frac{dH_2}{dt} = \frac{u^*}{r_g}\left(H_1 - \frac{H_2}{H_{sat}}\right) \tag{2.5}$$

---

with the following component equations:

$$B = G\alpha[I](1-n)(1-bC)(1-bA) \tag{2.6}$$

$$\alpha[I] = \alpha_0\left(\frac{I}{I_0}\right)^p \tag{2.7}$$

$$m[\Phi] = \begin{cases} 1 & \text{if } \Phi < \Phi_{on}, \Phi > \Phi_{off} \\ 0 & \text{if } \Phi_{on} \leq \Phi \leq \Phi_{off} \end{cases} \tag{2.8}$$

$$\Phi[A, C] = \arctan\left(\frac{A}{C}\right) \tag{2.9}$$

$$r[I] = 1 - r_a \left(\frac{1}{1 + \exp\left(-\frac{(I - r_b)}{r_c}\right)} \right) \tag{2.10}$$

$$M[H_2] = \frac{M_{max}}{1 + \exp\left(\frac{H_{sat} - H2}{\sigma}\right)} \tag{2.11}$$

Parameters are outlined next. Specific parameter values are listed in Table 2.1.

Table 2.1 Parameter Values

h	$\frac{\pi}{12}$	μ	0.23	r_c	26
G	33.75	q	$\frac{4}{3}$	Φ_{on}	-1.44
α_0	0.05	k	0.55	Φ_{off}	2.78
I_0	9500	γ	60	τ_{H_1}	3.11
b	0.4	β	0.0075	u^*	4700
σ	50	r_a	0.94	r_g	0.9
H_{sat}	325	r_b	110	I	input
p	varies	$\tau_{\mathbf{C}}$	varies	**Mmax**	varies

All parameters assigned with the exception of p, τ_C, and $Mmax$ which are the focus of the Thesis. p varies from $.2 - 2$. τ_C varies from $23.5 - 24.7$. $Mmax$ varies from $0 - 1$. I is the input into the system. Standard values are $\tau_C = 24.2$ and $p = 0.5$. Note that values of Φ_{on}/Φ_{off} shown here are for results in Chapter 3. Chapter 4 uses different values of Φ_{on}/Φ_{off} which are specified there. All other values remain the same.

2.1.1 Variable and Parameter Descriptions

I is the input for the system. It is light in lux. We use 4 discrete values 0, 100, 1,000, and 10,000. To simplify the simulations, values persist for the entire hour to which it is assigned.

The variables of the model are C, A, n, H_1, and H_2. C is the primary circadian variable and corresponds with Core Body Temperature (CBT). A is an auxiliary

variable that mathematically complements C. n tracks the process of activation and inactivation of the photosensitive retinal proteins. It ranges strictly from 0 to 1. H_1 simulates the pineal gland's generation of melatonin. H_2 is the concentration of melatonin in blood plasma in $pmol/L$. The parameter H_{sat} establishes a theoretical maximum for H_2 although with the other parameters, actual maximum is significantly below H_{sat}.

We vary the following parameters throughout the thesis: τ_C; p; and $Mmax$. τ_C is the intrinsic circadian period. It is the time it takes for the limit cycle given light input of 0 to complete one cycle. We vary it from 25.3 to 24.7 in increments of .1 excluding 24.1. p is sensitivity to light. We vary it from 0.2 to 2 in alternating increments of 0.3 and 0.2. $Mmax$ scales the feedback from the melatonin system to the circadian system. We vary the parameter from 0 to 1 in increments of 0.1.

The component equations of the model are B, $\alpha[I]$, $m[\Phi]$, $\Phi[A, C]$, $r[I]$, and $M[H_2]$. B is the direct drive which increases instantly in response to increased light input. It generates a spike before decreasing to an equilibrium intermediate to its previous value and the spike value. $\alpha[I]$ is the rate at which inactivated retinal photosensitive proteins are activated given a particular light input. $m[\Phi]$ controls the melatonin generation period. Melatonin generation starts at Φ_{on} and stops at Φ_{off}. The given values of Φ_{on} and Φ_{off} corresponds with a melatonin generation range of just under a third of the limit cycle on the lower left portion (see Fig. 3.1). Φ is the phase of the circadian pacemaker treating A as y and C as x. $-\pi < \Phi <= \pi$ where Φ decreasing except when $A = 0$ and $C < 0$ when Φ transitions from negative to positive. Note that in our python code, Φ is computed as np.atan2(y,x). $r[I]$ is the effect of light on melatonin generation. Observe that melatonin generation decreases with increasing light intensity due to $r[I]$. $M[H_2]$ is the feedback term from the melatonin system (equations (2.4) and (2.5)) to the circadian system via equations

(2.1) and (2.2). Note that further references to the component equations are made without their inputs. For example, $M[H_2]$ is referred to as M.

What remains are the constant parameters. h scales both A and C. γ scales n. G scales the direct drive. k further scales the direct drive. b is a coefficient for the circadian variables on the direct drive. μ modifies how quickly the oscillator returns to its limit cycle after perturbation. q is a coefficient chosen to work with other coefficients to yield an amplitude of 1 for the limit cycle at standard values of τ_C and p. β is the rate at which the active retinal photosensitive proteins are inactivated. α_0 is the rate at which inactivated retinal photosensitive proteins are activated. I_0 scales the effect of light input. Φ_{on} = fon is the phase of the circadian pacemaker at which melatonin generation begins. Φ_{off} = foff is the phase of the circadian pacemaker at which melatonin generation ends. Note that fon and foff (pronounced 'eff-on' and 'eff-off') appear frequently in the plots. They are simply code names for Φ_{on}/Φ_{off}. r_a, r_b, and r_c are "parameters of the sigmoid function obtained by fitting to experimental data" ([1],pg. 4). H_{sat} is the concentration of melatonin in blood plasma at which it is saturated. σ controls the steepness of the sigmoid $M[H_2]$. τ_{H_1} is the time constant for pineal gland melatonin generation. $u*$ is the equilibrium rate at which aMT6s is eliminated. r_g is the fraction of melatonin converted into its metabolite aMT6s.

2.1.2 Light Input

To simplify the model, the we use a standard 24-hour distribution of light. We assign $I = 100(1000)100[0]$ which represents the intensity of light in lux. The corresponding time, $N = 1(12)4[7]$ indicating the 1st hour has an input of 100 lux light, followed by 12 hours of 1,000 lux light, followed by 4 hours of 100 lux light where the remaining 7 of the 24 hours have an input of 0 lux light (darkness). Note that we refer to periods of 0 lux light as 'Night Hours', periods of 100 lux light as 'Indoor Hours', periods of

1,000 lux light as 'Day Hours'. Additionally, periods of 10,000 lux light are referred to as 'Bright Hours'.

2.1.3 Model Description

The entire model is composed of three related models. The Forger-Jewett-Kronauer model (**FJK Model**) [7, 10] An updated version of Kronauer's model of light-based circadian rhythm. It is a 3-dimensional model which combines a 2-Dimensional coupled circadian pacemaker with a 1-dimensional model of light activated retinal activity [14]. In this formulation of the FJK model, the minimum CBT time is indistinguishable from the time at which C reaches its minimum [7]. Note that the proceeding models use some formulation of the FJK model as the circadian component. The current model uses the version present in the work of Diekman and Bose along with the parameter values [5].

Unified Model of melatonin [1]. It is a melatonin model which simulates the melatonin cycle based on light intensity and phase of the circadian cycle. The model is special for two important reasons. First, the amount of melatonin inhibition corresponds with the intensity of light. Further, the concentration of melatonin is allowed to gradually reduce as opposed to instantly assuming its new equilibrium value. Second, the model simulates excretion of melatonin through saliva and via metabolization into aMT6s (6-sulfatoxymelatonin) and subsequent disposal via the urinary tract. Note that there are additional equations describing aMT6s behavior of which the current model does not take advantage. These equations are readily available. However, one should keep in mind that u^* has been changed.

Exogenous Model of melatonin [2]. A melatonin model intended to predict the behavior of melatonin introduced into the body from an external source. The part of the Exogenous Model of particular concern to the current model is a mathematical term, M, which uses melatonin concentration in blood plasma to dictate feedback in

to the FJK model. The ways in which this M term interacts with the rest of the system is a primary component of the thesis.

The model fits together conceptually as in Fig 2.1. Light is registered by the system via the retina. The retina detects the light and sends signals to the SCN. The SCN processes the signals and in turn sends inhibitory signals to the pineal gland corresponding with both the phase of the circadian pacemaker (via $\Phi[A, C]$) and the intensity of light (via $r[I]$). The pineal gland generates melatonin and deposits it into the blood. The concentration of melatonin in the blood modifies the circadian pacemaker (via $M[H2]$).

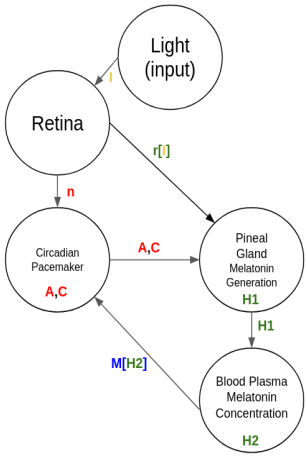

Figure 2.1 Model Flow Chart. Schematic diagram of the model. Variables or functions are colored by component model membership. Yellow is independent and reserved for input. Red is for the FJK model. Green is for the Unified Model of melatonin. Blue is for the Exogenous Model of melatonin. The input into the system is light I. Photosensitive proteins react to the light resulting in a signal to the SCN. n simulates the population of active and inactive photosensitive proteins and influences the activity of A and C of the FJK model. The SCN sends an inhibitory signal to the pineal gland directly related to the intensity of light via $r[I]$ and the phase of the circadian pacemaker ($\arctan(A, C)$) dictates whether the pineal gland generates melatonin or not. The pineal gland generates melatonin H_1 and the melatonin concentration in blood plasma H_2 increases. H_2 influences the activity of the circadian pacemaker via $M[H_2]$.

2.2 Things to Keep in Mind

The model of the thesis was painstakingly assembled. However, while the component models are largely as they appeared in their respective articles, we have made changes. Most notably, we chose to omit the scalar parameters present in the Exogenous Model on the M term in equations (2.1) and (2.2). We chose to vary $Mmax$ from 0 to 1 while the authors of the Exogenous Model set it to a constant 0.019513.

We multiplied the parameter u^* in equation (2.5) by 10,000 in order to achieve expected model behavior (i.e. the Unified Model had $u^* = 0.47$ whereas this model uses $u^* = 4700$).

Furthermore, both the Unified Model and the Exogenous Model had a circadian component based on some version of the FJK model. Authors of their respective models also chose parameters convenient to them. The model of this thesis use a slightly modified version of the FJK model with parameters used in Diekman and Bose's work on Entrainment Maps.

We wrote all programs for the thesis in python. Programs are designed to use comma separated value files as input and to create them as output in order to take advantage of high-performance computing resources available via Lochness. For a sense of the scope of the programs, computing the limit cycles for all combinations of parameters for $\tau_C \geq 24.2$ took around six hours. We computed 18 of these. One for each hour of bright light and one without bright light. On the other hand, the programs that compute the entrainment maps take just under 24 hours for the same set of parameters. Likewise, we computed 18 of these. While the time to run was the same on Lochness, we were able to run all 18 in parallel which saved countless days of computation time and enabled this thesis to be completed in a reasonable time.

Lastly, the results of the thesis are theoretical and have not been tested with real-world data.

CHAPTER 3

ENTRAINMENT MAPS

In this chapter, we assess the entrainment maps of various combinations of τ_C, p, and $Mmax$. τ_C varies from $25.3 - 24.7$ in increments of 0.1 excluding 24.1. p varies from $0.2 - 2$ in alternating increments of 0.2 and 0.3. $Mmax$ varies from $0 - 1$ in increments of 0.1.

The first section deals with the limit cycles resulting from the model. The next section considers the effect of $Mmax$ on the the shape of the limit cycle. The third section details the process for computing the entrainment map which consists of finding ρ and then finding Π. The fourth section introduces the plots and walks through two cases of entrainment map evolution with and without bright light. The fifth section discusses a number of results which lay the groundwork for the next section. The sixth section displays all of the combinations of parameters in the form of heat maps considering the administration of bright lights at different times. Details are in the next section.

3.1 Limit Cycles

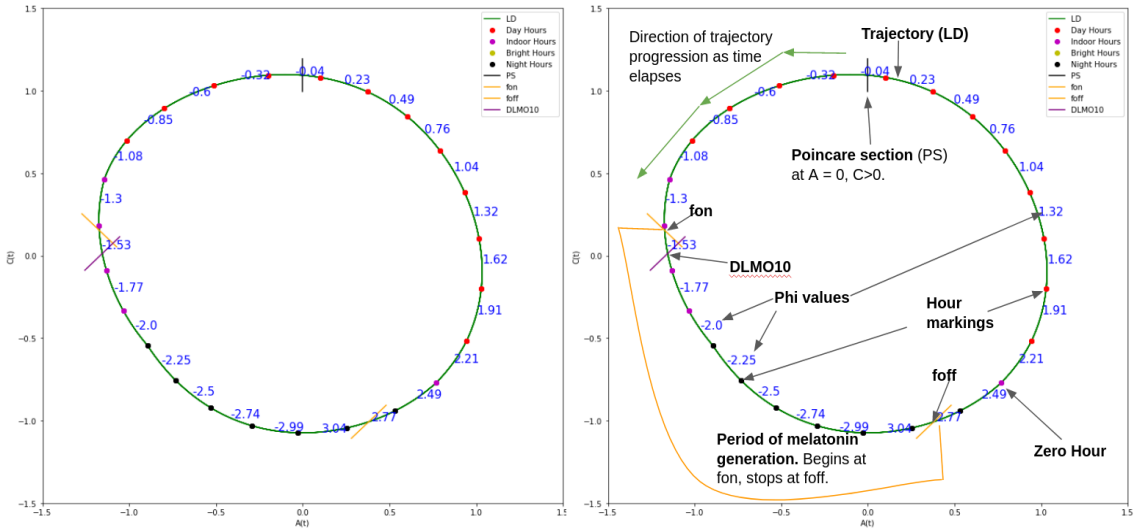

Figure 3.1 Anatomy of a Limit Cycle. Uses standard values of τ_C and p with $Mmax = 0$. Left plot shows the limit cycle without the clutter. Right plot explicitly identifies components of the graph. LD is the **trajectory** of the model. It progresses counter-clockwise with increasing time. The **Poincare section** is the black vertical line at $A = 0$,$C > 0$. It serves as the initial conditions for the model and rho is computed by changing the phase of light and noting when the trajectory returns to the Poincare section. **fon** $= \Phi_{on}$ and is the position at which melatonin generation starts. **foff** $= \Phi_{off}$ and is the position at which melatonin generation stops. However, note that H_2 reaches its max at either foff or the start of an hour of increased light. After foff, H_2 gradually decreases to obtain a min value sometime before the trajectory reaches fon again. **Phi values** are values of Φ. Note that $\Phi = 0$ at the Poincare section at the top of the limit cycle and it progresses to $-\pi$ at the bottom of the limit cycle at which point it decreases from pi back to 0. Phi values are printed at every half-hour. **Hour markings** represent the hours and are color coded to represent the intensity of light during that hour. There are four intensities of light. Only 3 are shown here: Day Hours = 1,000 lux; Indoor Hours = 100 lux; Night Hours = 0 lux. The fourth intensity if bright light represented by Bright Hours with intensity 10,000 lux. **Zero Hour** represents the very first moment of the 24 hour day. It is also represents the mark for the end of the previous day. It is always a lone Indoor Hour unless we mention the effects of BLT at hour 1. In that case, it is a Bright Hour.

The plot of a limit cycle is described in detail in Fig. 3.1. Additionally, the figure shows a visualization of an entrained limit cycle. Note that the plot displays 72 hours of simulation with light values plotted as color coded dots at every hour. Observe

that only 24 dots are visible indicating that the dots are plotted at the exact same position every cycle.

For comparison, observe the non entrained limit cycle in Fig. 3.2. Neither the dots nor the trajectory overlap. Observe in this case that from day to day, the position of the dots retreat a small amount. Note that after a sufficient amount of time, the dots will have retreated enough to the point where they will overlap with the current representation. Since the hours of light intensity transition along the limit cycle, there will be different melatonin profiles due to $r[I]$ (equation 2.10). That is, changing light intensity times along the limit cycle corresponds to changing light intensities within the melatonin generation period (from fon to foff) and due to the action of $r[I]$ this results in a different amount of melatonin generated from day to day.

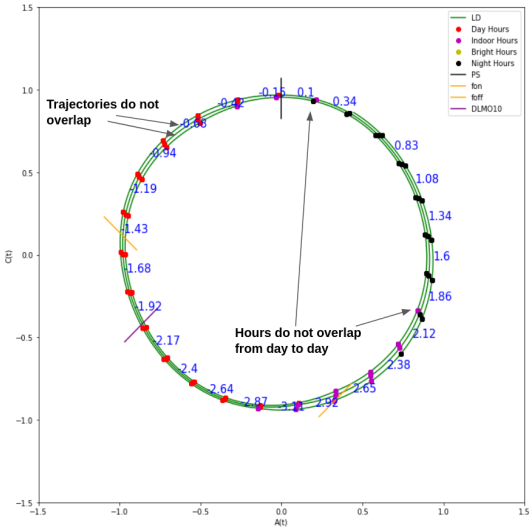

Figure 3.2 Non-entrained Limit Cycle. This shows three days of model simulation. Note that the trajectory and the hour markings do not overlap consistently. Furthermore, the hour markings are at least an hour off from day to day. The lack of overlap means that from the day to day, the representation shifts, and the Night Hours eventually take place within the period of melatonin generation which will significantly impact the position of DLMO10. Likewise, eventually the relative positions will return to this representation, resulting in the current position of DLMO10. That means the melatonin profile is constantly changing.

Note: Plots of limit cycles frequently include legends with 'Bright hours'. This is done to standardize the plots and is not indicative of the presence of bright light in the simulation. The presence of bright light is mentioned explicitly.

3.2 The Effect of $Mmax$ on Limit Cycles.

$Mmax$ has a distorting effect on a limit cycle for the model. One can see the effect in Fig. 3.3. In brief, the distortion is minimized around fon because that is when M is at its minimum value. On the other hand, the most distortion exists around foff because M achieves its maximum near there. The distortion can be explained using the nullclines in Figs. 3.4 and 3.5.

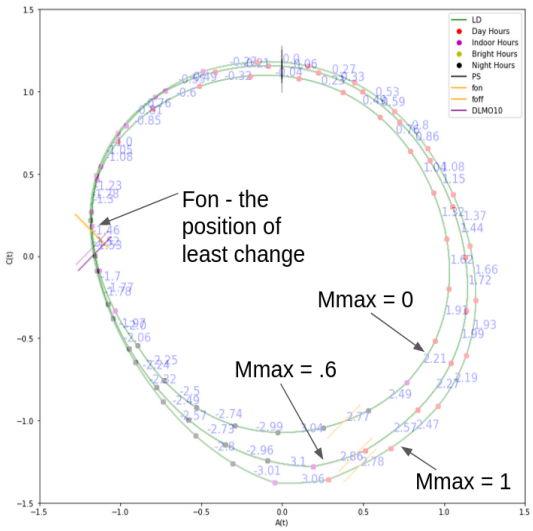

Figure 3.3 Limit Cycle Progression with Increasing Values of Mmax. Shows overlapping limit cycles with three different values of Mmax. Uses standard values of τ_C and p. Note that the least change takes place near fon and the most change takes place near foff. The difference is due to the evolution of M which is dependent on H_2. The value of H_2 is lowest around fon and increases until reaching a max value near foff. After foff, H_2 decreases steadily until fon. Increasing $Mmax$ multiplies M and amplifies its effect, resulting in the different limit cycle representations.

The C nullcline is the vertical nullcline defined by:

$$A = \frac{G\alpha[I](-1+n+.4C-.4Cn)+M}{(1+.4G\alpha[I](-1+n+.4C-.4Cn)} \tag{3.1}$$

The A nullcline is the cubic nullcline defined by:

$$C = \frac{\mu(A - \frac{4}{3}A^3) - M}{(\frac{24}{0.99669\tau_C})^2 + kB} \tag{3.2}$$

Note that parameter values in equations 2.12 and 2.13 are identical to those in the rest of the model. Additionally, n and B are treated as a constants and take the values $n(t)$ and $B(t)$. Figs. 3.4 and 3.5 show the nullclines of the simulation at every hour with the complete 24-hour trajectory starting at Zero Hour (see Fig. 3.1 for definition) and the position of the trajectory at the time the nullclines were computed. Additionally, it shows the nullclines of a limit cycle where $Mmax = 1$ in red and the nullclines of a limit cycle where $Mmax = 0$ in blue for reference. The position of the red plots corresponds to the value of M which is directly related to the value of H_2. So, times when the red and blue plots are most different correspond to times when melatonin concentration in blood is highest.

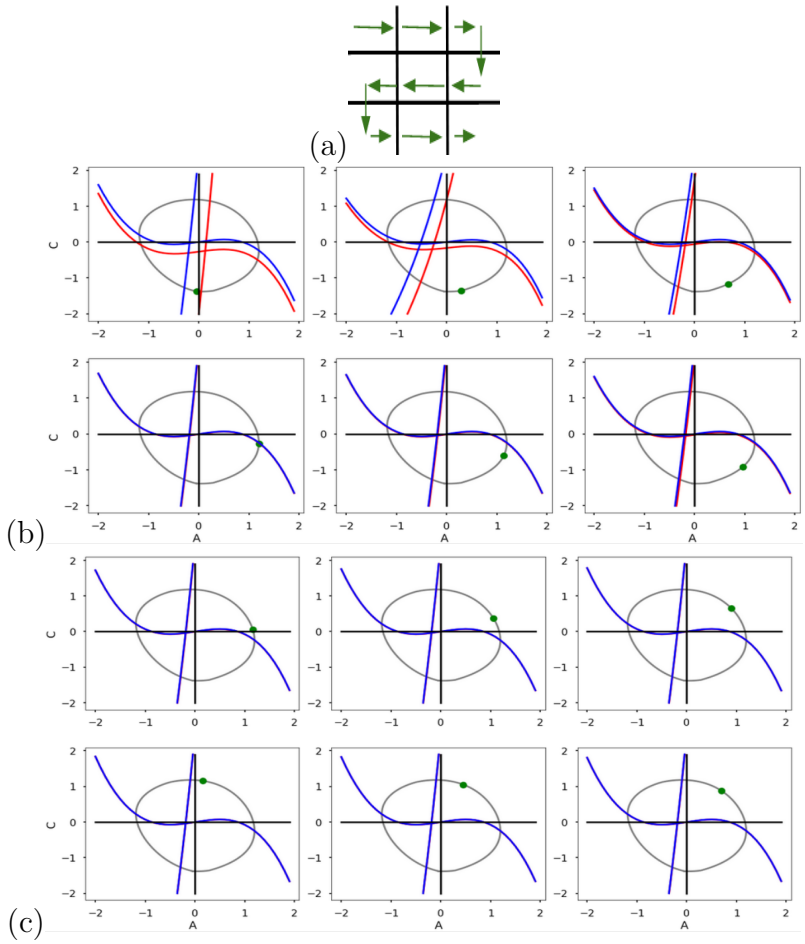

Figure 3.4 Nullcline Evolution over 24 Hours (1st half). (a) Shows the order of evolution. Starting from the top left in (b), transition right. In the next row, start right, transition left. Red plots are A and C nullclines when $Mmax = 1$. Blue plots are A and C nullclines when $Mmax = 0$. Presence of just the blue plot indicates that red and blue plots overlap. The grey plot is the trajectory over a 24 hour period. The green dot is the position of the trajectory at time t.

Observe that in this case (using standard values of τ_C and p), blue and red plots are significantly different for the first few hours in Fig. 2.5. Then, in Fig. 2.6., they are practically indistinguishable for many hours until the final few hours.

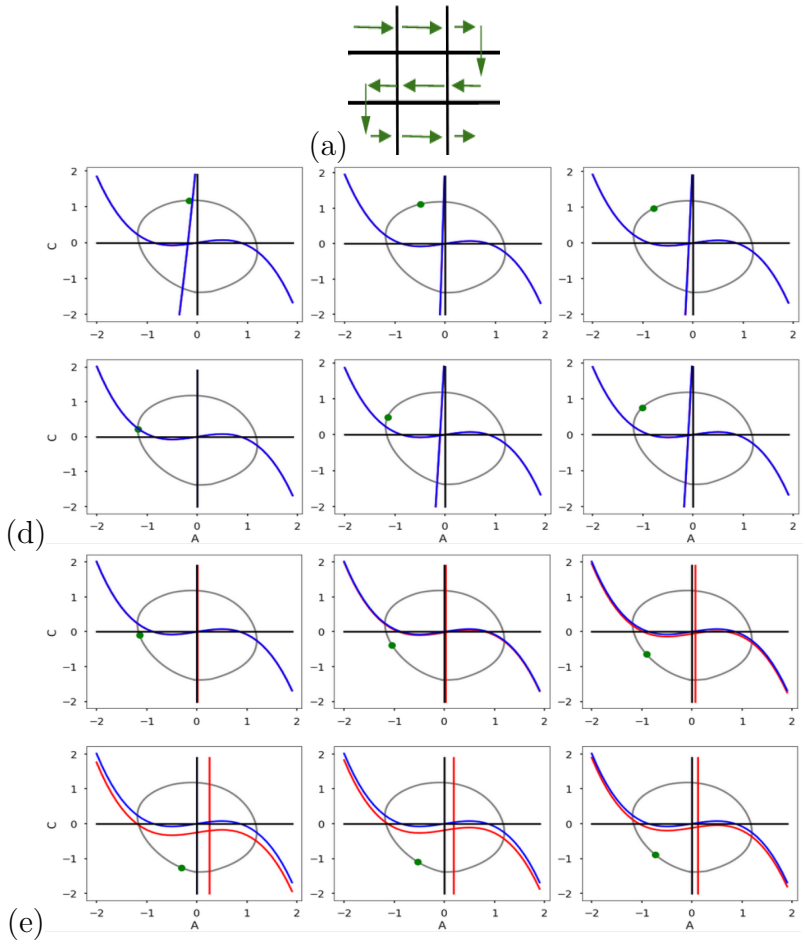

Figure 3.5 Nullcline Evolution over 24 Hours (2nd half). (a) Shows the order of evolution. Starting from the top left in (d), transition right. In the next row, start right, transition left. Red plots are A and C nullclines when $Mmax = 1$. Blue plots are A and C nullclines when $Mmax = 0$. Presence of just the blue plot indicates that red and blue plots overlap. The grey plot is the trajectory over a 24 hour period. The green dot is the position of the trajectory at time t. Additionally, in the top left of (e) the absence of blue and red vertical nullclines means that they overlap with the y-axis. The last 7 hours is when the vertical nullcline is perfectly vertical and corresponds with the hours when $I = 0$.

It is the handful of hours when the red and blue plots are different that dictate the distortion apparent in Fig. 2.4. Furthermore, the hours when the red plot is furthest removed from the blue plot correspond with the periods of largest distortion on the limit cycle.

3.3 Computing the Entrainment Map

Entrainment Maps are a result of work by Diekman and Bose [4–6]. The process requires that one first compute ρ by establishing a Poincare section and computing a trajectory from that section iteratively after changing the phase of light by predetermined amounts.

3.3.1 Phase of Light (Computing ρ)

The phase of light refers to the order of light input. To change the phase of light, consider N. 'Remove' some interval from the value on the left and move that value to the right. Note that the corresponding value of I must be preserved. The below table shows how to change the phase of light.

Table 3.1 Computing the Phase of Light

Phase	N	I
0	1(12)4[7]	100(1000)100[0]
1	.9(12)4[7].1	100(1000)100[0]100
2	.8(12)4[7].2	100(1000)100[0]100
...	...	...
11	(11.9)4[7]1(0.1)	(1000)100[0]100(1000)
12	(11.8)4[7]1(0.2)	(1000)100[0]100(1000)
...	...	...
240	[.1]1(12)4[6.9]	[0]100(1000)100[0]
241	1(12)4[7]	100(1000)100[0]

We begin with the light profile which are the original values of N and I in Phase 0. We change the phase of light by adjusting the position of .1 hours from the left most value in N to the right, maintaining the lux value. Phase 1 shows the first step of the process. We remove .1 hours from the left most value which corresponds to 100 lux. We then add .1 hours of 100 lux to the right. Phase 2 is the identical process resulting in .2 hours of 100 lux on the right. After 10 iterations, we have moved a full hour from the left to the right and start on the next hour, taking .1 hours of 1000 lux from the left and moving it to the right. We repeat the process for another 229 iterations until the phase of light is identical to the original light profile. We stop after Phase 240 as at Phase 241 we arrive at the original light profile and our calculations would be redundant.

The initial phase of light is Phase 0 in the table (it is the original light profile). Run the simulation using the value of the limit cycle at the Poincare section as the initial values. Record the time it takes for the trajectory to return to the Poincare section. This is $\rho(x)$ where $x = 0$. Compute the next phase of light as in Phase 1 in the table and run the simulation again using the same initial values from the previous simulation and once again record the time it takes for the trajectory to return to the

Poincare section. Repeat this process for every phase of light until the phase of light is the same as the original light profile.

3.3.2 The Entrainment Map (Computing Π)

The Entrainment Map $\Pi(x)$ (where x is the phase of light which is the order of light input) is computed first by establishing a limit cycle, then by establishing a Poincare section somewhere along the limit cycle. Then starting the simulation at the Poincare section, record how much time elapses until the trajectory returns to the Poincare section. Repeat the process for every possible phase of light to obtain $\rho(x)$. A walk-through of the process to compute $\rho(x)$ can be found in the 'Phase of Light' section. $\Pi(x) = \rho + x$ and entrainment depends on whether or not there are values $\Pi(x) = x$. This corresponds to $\Pi(x)$ crossing the diagonal and $\rho(x)$ crossing the $\rho(x) = 24$ line. The map either crosses the diagonal twice, or does not intersect the diagonal. The first case yields stable and unstable fixed point and the value of the stable point is the time that it takes the limit cycle to reach the Poincare section after the lights have turned on. In this case, the combination of parameters are said to entrain. The second case results in no entrainment. There is a third case, where the map intersections the diagonal tangentially. It results in a saddle-node bifurcation point. Its presence indicates a value at which entrainment stops.

Note that plots represent Π as 'Pi' and ρ as 'rho'.

3.4 Entrainment Map Plots

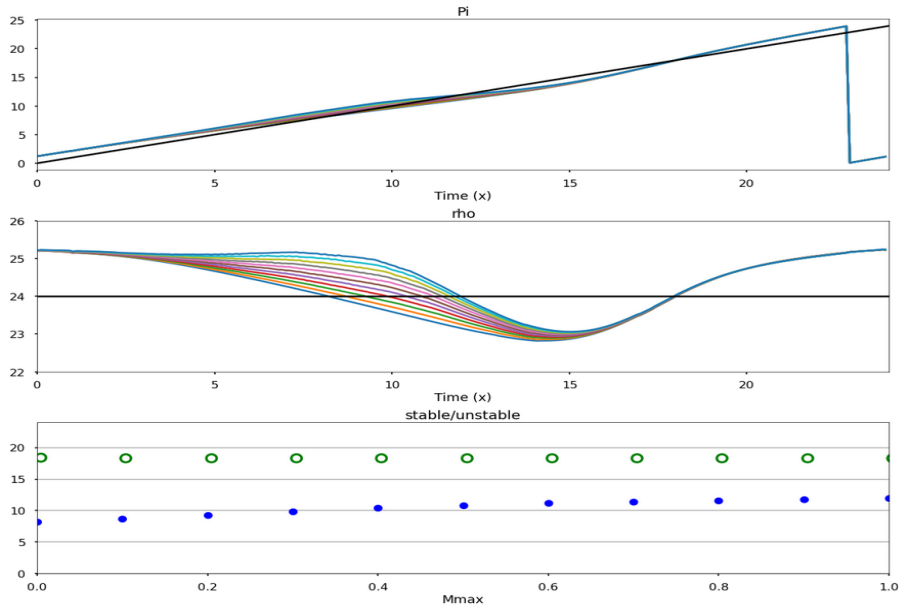

Figure 3.6 Pi and rho plots comparing $0 \leq Mmax \leq 1$ with BL in 1st Hour. Top: Pi plot. Diagonal (black line) is $\Pi(x) = x$. The x value is the time from when the lights first turned on. It also denotes the position of the phase of light. Dark blue is $Mmax = 0$ (lower)and $Mmax = 1$ (upper). Points where map intersects diagonal are stable or unstable. Middle: rho plot. Black line is 24 hours. Dark blue is $Mmax = 0$ (lower)and $Mmax = 1$ (upper). $Mmax = .1$ is just above $Mmax = 0$ and just below $Mmax = .2$ and the same relationship persists for all values of $Mmax$. Rho provides a more detailed view of the behavior of Pi. Note that the relative stable points are observable with rho whereas they are difficult to make out with Pi. Bottom: stable/unstable positions. Solid blue dots are stable points. Green circles are unstable points. Presence of stable and unstable points for any value $Mmax$ indicates entrainment for that value. Here, all values $0 \leq Mmax \leq 1$ entrain.

3.5 Entrainment Map Cases

In this section we cover specific entrainment results. Each plot includes results for all 11 values of $Mmax$. There are particular cases that are color coded in order to visualize the results using heat maps in the next section.

The black case, Fig. 3.7, is when there are no values of $Mmax$ for a particular combination of τ_C and p that entrain to 24 hours. Lack of entrainment is revealed by the fact that there are no maps which intersect $y = 24$ which corresponds to the case where there are no values where $\Pi(x) = x$.

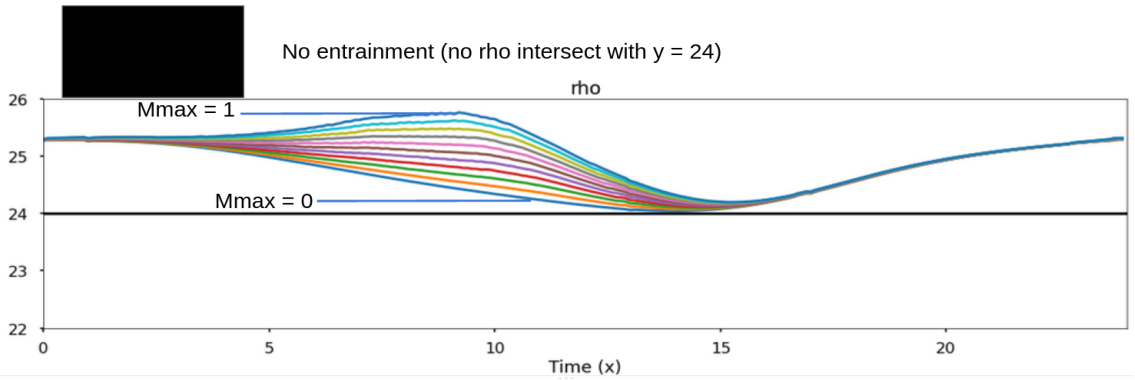

Figure 3.7 Entrainment Map Cases: No Entrainment (Black).

The red case, Fig. 3.8, is when there is one value of $Mmax$ for a particular combination of τ_C and p that entrains to 24 hours. Note that based on the way that the chosen values of τ_C, p, and $Mmax$ behave, the single value of $Mmax$ that entrains must be either $Mmax = 0$ or $Mmax = 1$. The color does not distinguish between the two possibilities. For this case, we used the bottom plot in Fig. 3.6 in order to determine that only one value entrains.

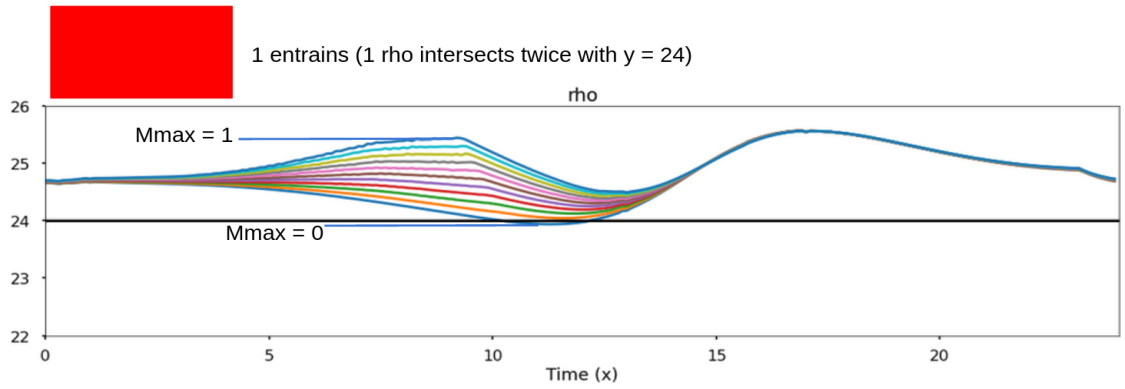

Figure 3.8 Entrainment Map Cases: 1 Entrains (Red).

The orange and yellow cases, Figs. 3.9 and 3.10, are related to the red case, but involves higher numbers (2-4 and 5-10 respectively) values of $Mmax$ entrain to 24 hours for a particular combination of τ_C and p. As in the red case, these cases include both instances when higher values of $Mmax$ entrain or lower values of $Mmax$

entrain. In these cases, it is necessary to use the bottom plot in Fig. 3.6 in order to determine which values entrain.

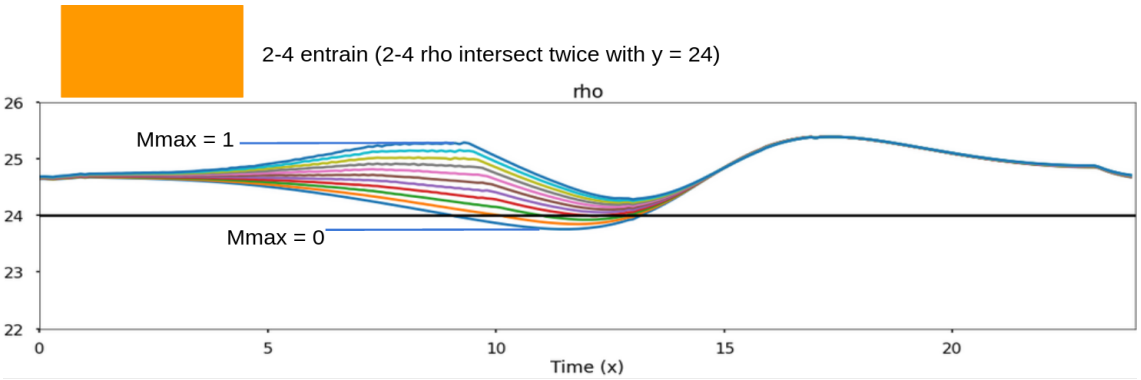

Figure 3.9 Entrainment Map Cases: 2-4 Entrain (Orange).

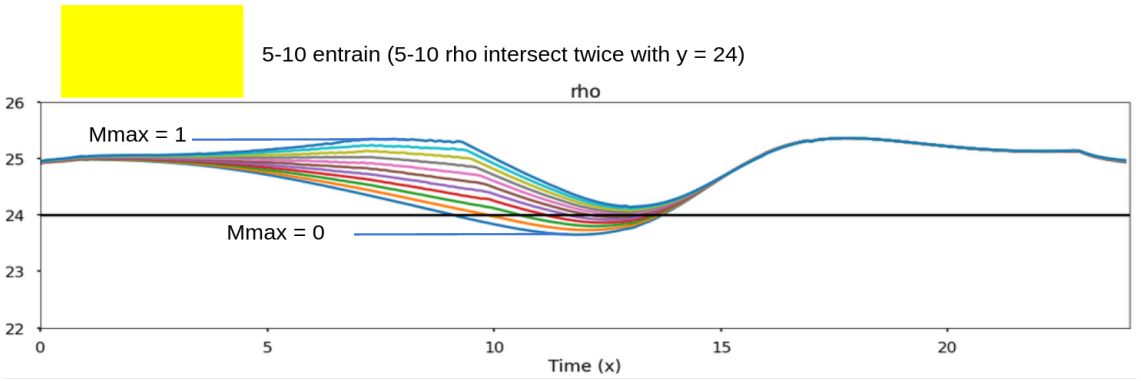

Figure 3.10 Entrainment Map Cases: 5-10 Entrain (Yellow).

The green case, Fig. 3.11, is when all values of $Mmax$ entrain to 24 hours for a particular combination of τ_C and p. Often this is apparent through visual inspection of rho, but can include cases where the portion that intersects $y = 24$ is the portion where all of the values are practically indistinguishable. This can lead to the need to verify using the bottom plot in Fig. 3.6 in order to determine which values entrain.

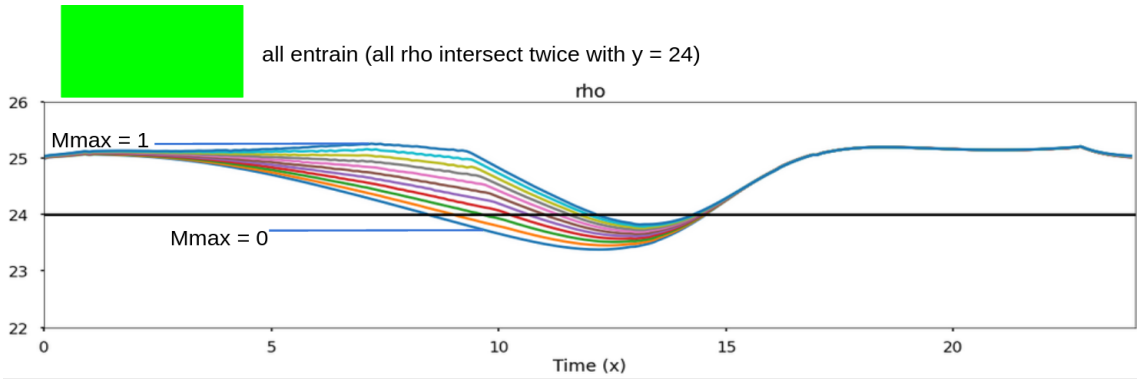

Figure 3.11 Entrainment Map Cases: All Entrain (Green).

The magenta case, Fig. 3.12, is when some values of $Mmax$ establish two stable points and two unstable points. This necessarily entails entrainment to 24 hours for those values, but which time the Poincare section adopts is dependent on the initial phase of light (x). That is, if the phase of light starts at a time to the right of either of the unstable points, the time of the Poincare section ends up entraining to the value of the stable point to the right of the unstable point. Likewise, Poincare section entrains to the stable point to the left of the unstable point if the phase of light begins on the left.

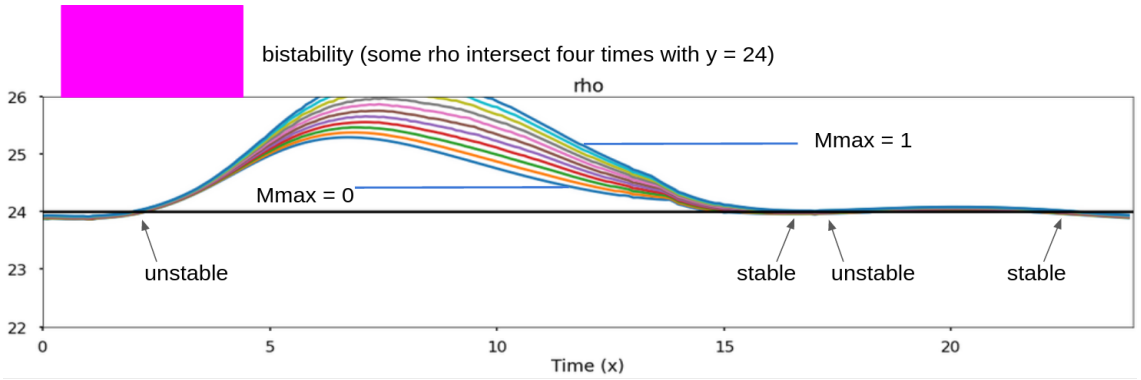

Figure 3.12 Entrainment Map Cases: Bistability (Magenta).

There are additional bistability cases presented in the Entrainment Map Heat Maps for $\tau_C \leq 24$. They are represented as shades of magenta. However, presenting them here would be redundant considering they are analogous to the red, orange,

and yellow cases in terms of denoting the number of $Mmax$ values that demonstrate bistability.

Furthermore, blue represents tristability which involves yet another stable and unstable point. It is unclear whether this is real or an anomalous result due to the way the code works.

3.6 Entrainment Map 'Heat Maps'

The Entrainment Map Heat Maps provide a method for quick assessment of the evolution of entrainment as the time of bright light administration progresses hour by hour. The heat maps consist of 6x8 blocks corresponding with combinations of τ_C (along the columns) and p (along the rows). The colors correspond to the numbers of $Mmax$ values which entrain. The colors are defined and described in the previous section. Note that the evolution of bright light progresses in a snake like manner starting with bright light administered at hour 1 ('BL hr1') in Figs. 3.8 and 3.10 and 'BL hr10' in Figs. 3.9 and 3.11.

The heatmaps show that for a long τ_C, the time of bright light with the most entrainment is hour 5. In fact, in general, morning hours (Fig. 3.13) are best for long τ_C. Later hours (Fig. 3.14) introduce complications in the form of bistability that may be best avoided (see the magenta case, Fig. 3.12).

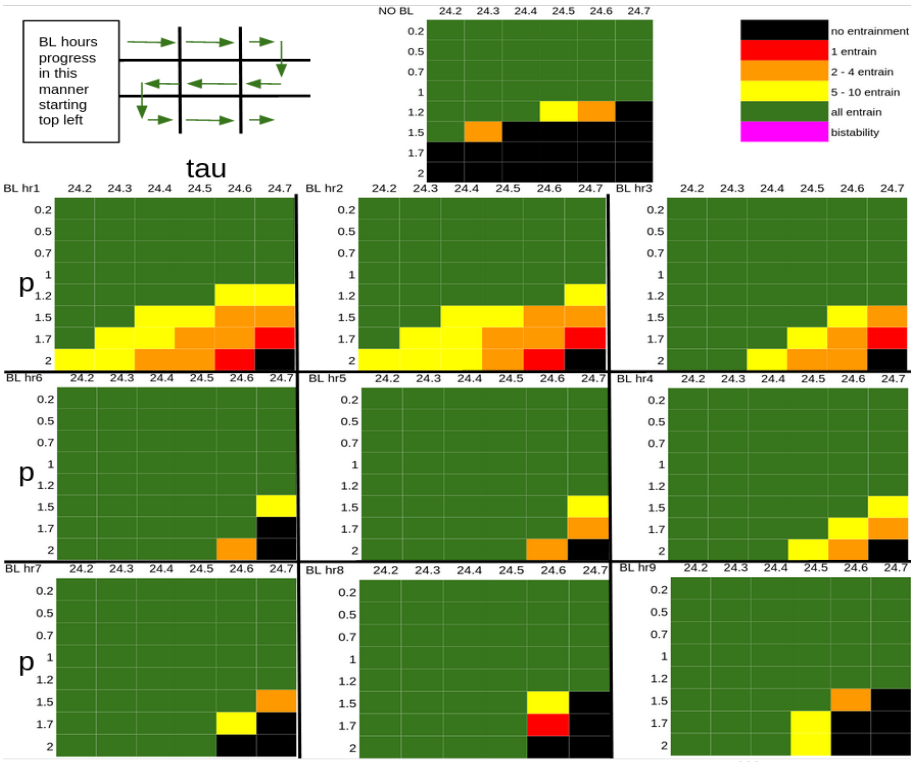

Figure 3.13 Bright Light Heat Maps: $\tau \geq 24.2$, Early Bright Light. Shows entrainment map results from hour 1 to hour 9. The heat map at the top shows the results of entrainment maps without bright light. The color denotes the results of different values of $Mmax$. Values of τ_C are columns and increase from left to right. Values of p are rows and increase from top to bottom. The diagram on the top left denotes the progression of bright light times starts on the heat map at top left, progresses to the right, progresses to the next row at the same column and progresses to the left. The next row then progresses left to right. Observe that hour 5 of bright light maximizes green cases (all $Mmax$ entrain) and minimizes black cases (no $Mmax$ entrain). From this perspective, administering bright light at hour 5 is preferable to other times for a long τ_C.

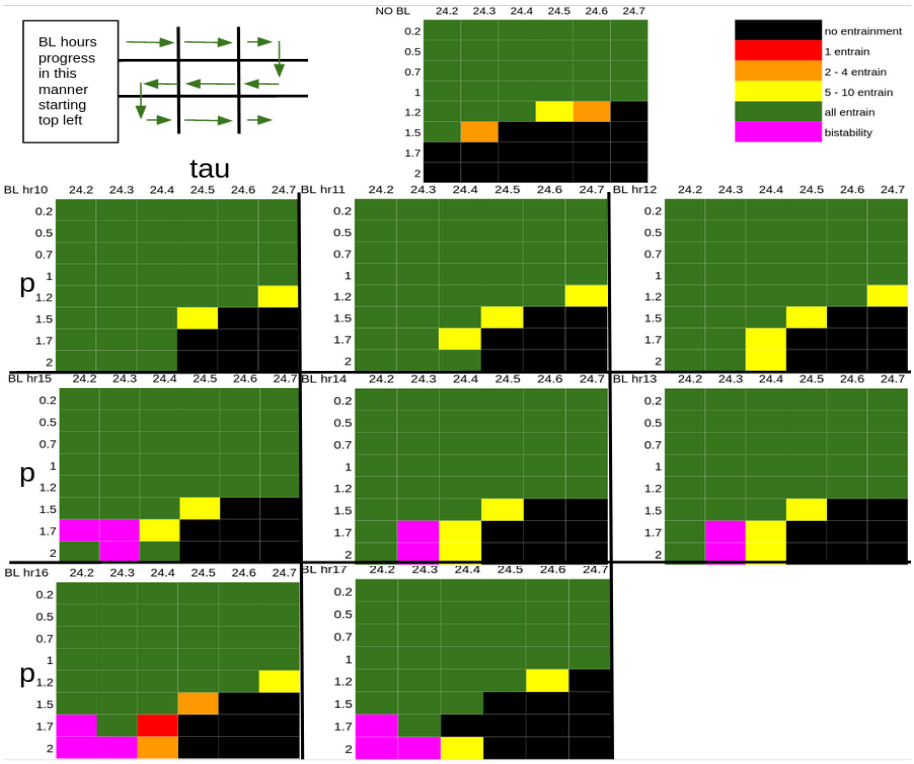

Figure 3.14 Bright Light Heat Maps: $\tau \geq 24.2$, Late Bright Light. Shows entrainment map results from hour 10 to hour 17. The heat map at the top shows the results of entrainment maps without bright light. The color denotes the results of different values of $Mmax$. Values of τ_C are columns and increase from left to right. Values of p are rows and increase from top to bottom. The diagram on the top left denotes the progression of bright light times starts on the heat map at top left, progresses to the right, progresses to the next row at the same column and progresses to the left. The next row then progresses left to right.

For a short τ_C, morning hours (Fig. 3.15) introduce complications and later hours (Fig. 3.16) entrain all of the combinations without the bistability.

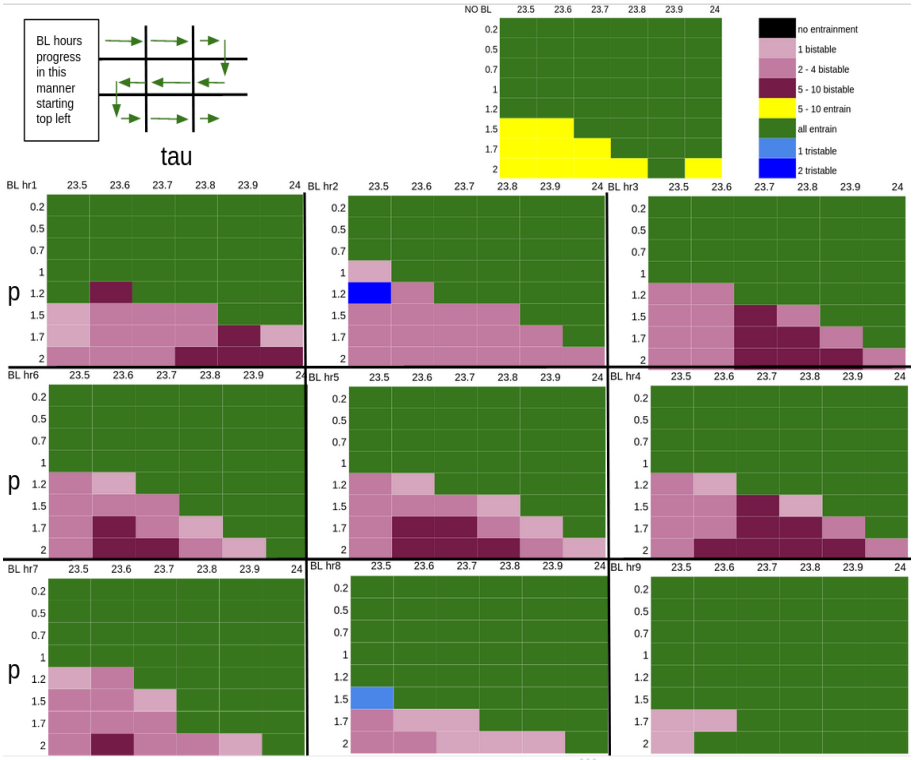

Figure 3.15 Bright Light Heat Maps: $\tau \leq 24$, Early Bright Light. Shows entrainment map results from hour 10 to hour 17. The heat map at the top shows the results of entrainment maps without bright light. The color denotes the results of different values of $Mmax$. Values of τ_C are columns and increase from left to right. Values of p are rows and increase from top to bottom. The diagram on the top left denotes the progression of bright light times starts on the heat map at top left, progresses to the right, progresses to the next row at the same column and progresses to the left. The next row then progresses left to right. Observe that all combinations entrain. The issue for these combinations of τ, p, and $Mmax$ are the cases of bistability. It is not obvious how to interpret this bistablity, but it appears to defeat the purpose of a global time-keeping mechanism to tend towards 2 different times depending on the phase of light at which the system starts. So assuming that bistability is a negative result for the circadian rhythm (and the same for tristability), these morning hours of bright light are not optimal for short τ_C.

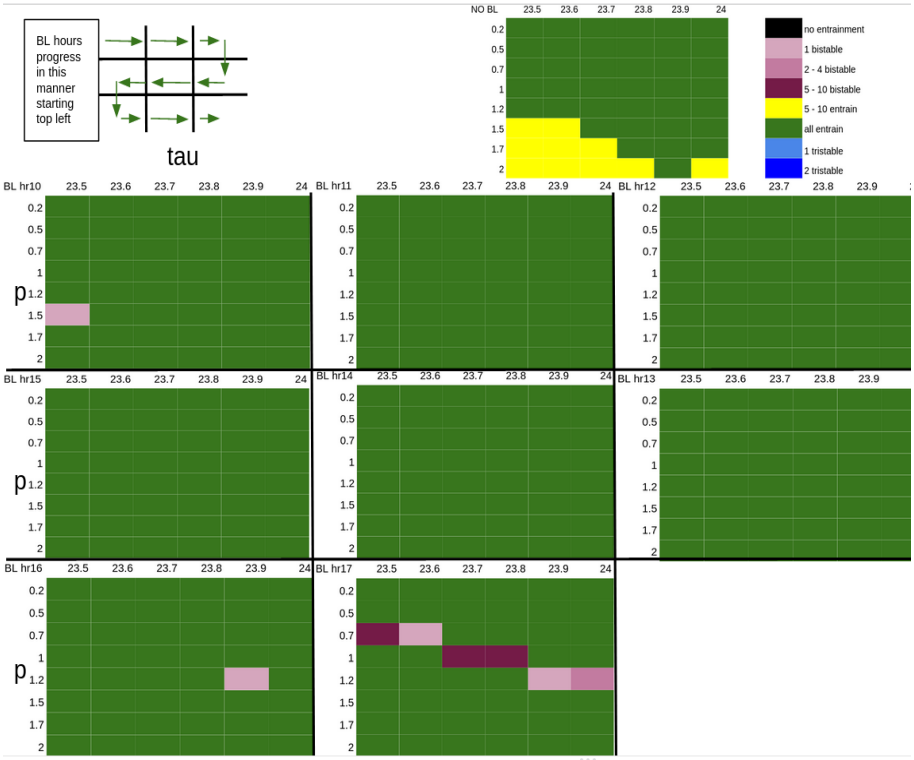

Figure 3.16 Bright Light Heat Maps: $\tau \leq 24$, Late Bright Light. Shows entrainment map results from hour 10 to hour 17. The heat map at the top shows the results of entrainment maps without bright light. The color denotes the results of different values of $Mmax$. Values of τ_C are columns and increase from left to right. Values of p are rows and increase from top to bottom. The diagram on the top left denotes the progression of bright light times starts on the heat map at top left, progresses to the right, progresses to the next row at the same column and progresses to the left. The next row then progresses left to right. Note that hours 11-15 exhibit entrainment for all combinations without any bistability. Using this perspective, it is preferable to administer bright light in these later hours.

The next chapter demonstrates that the heatmaps are not the only consideration one should have for how best to administer bright light. For instance, despite the fact that most combinations entrain in bright light administered during hour 5, the resulting limit cycle may not possess expected relationships such as the time between H_2max and $CBTmin$.

CHAPTER 4

'RESCUE' DEPRESSION WITH BRIGHT LIGHT CASE STUDIES

Note that in this chapter, we consider limit cycles computed using modified values of ϕ_{on}/ϕ_{off}. In these chapters we assign the values:

$$\phi_{on} = -0.94$$

$$\phi_{off} = -2.78$$

As usual, the orange lines depict both order of their arrival along the limit cycle as it progresses counter-clockwise. The parameters are referred to as 'fon' and 'foff' (pronounced 'eff-on' and 'eff-off') throughout the chapter corresponding with their plot labels and how we deal with them in the python codes.

This change was necessary in order to find any of the cases we observe in the chapter. For more information, see Fig. 4.2.

4.1 What is Rescued?

There is evidence that a particular subset of depressed patients may demonstrate a long τ_C due to a mutation in one of the genes involved in the biochemical processes in neurons in the SCN that governs periodicity of the circadian rhythm [11]. Assuming this is the case, we restrict our attention to cases of long τ_C and propose that there are cases of depression corresponding to some long τ_C combined with a p and $Mmax$.

We believe that entrainment to 24 hours is an essential component of BLT. However, it appears that there are more conditions that need to be met in order for BLT to be considered helpful. One condition seems to be the time between maximum blood melatonin (H_2max) and the minimum core body temperature. Note that $Cmin$ corresponds directly to the minimum core body temperature using this

rendition of the FJK model. H_2max occurs sometime in the middle of the sleep period and $Cmin$ occurs approximately 1.3 to 1.7 hours afterwards also during the sleep period [8]. That means there needs to be a period of sleep before H_2max and after $Cmin$. More specific constraints and a visualization of the conditions are provided in Fig. 4.1. If in addition to being entrained after the administration of bright light these conditions are met, the parameter combination is said to have been 'rescued.' The verb 'rescue' refers to the act of administering bright light to such a parameter combination. 'Healthy' means that the limit cycle meets the criteria for rescued without bright light. 'Needs rescuing' expresses the fact that an entrained limit cycle does not meet the conditions for having been rescued. It does not indicate that there is any possibility of rescuing the limit cycle.

Consideration of the relationship between H_2max and $Cmin$ and the length of the intrinsic period is the extent of our simulation of depression. As our model stands, it is unable to represent melatonin profiles in the way that we have come to understand. As such, 'depression' is a stand-in for a malady associated with circadian pacemaker.

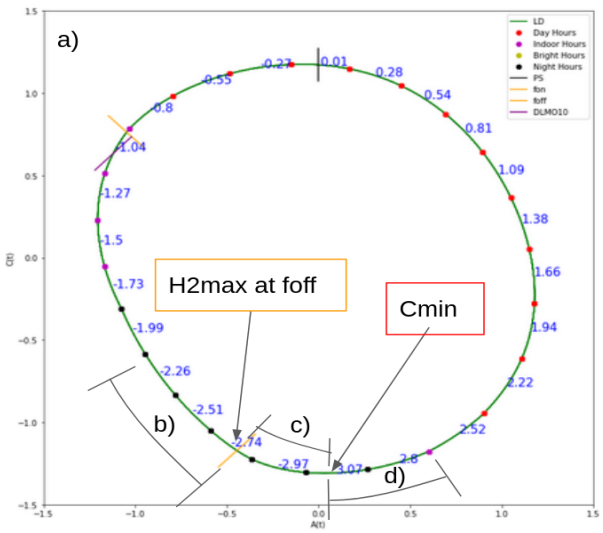

Figure 4.1 What it means to be rescued. Depicts visually the requirements for a limit cycled to be considered 'rescued.' a) The Limit cycle entrains; b) There are two or more Night Hours before H_2max (located at foff during Night Hours); c) There are 1.3-1.7 Night Hours between H_2max and $Cmin$; d) $Cmin$ occurs at least one hour before lights-on. Conditions based on the figure in Hickie et al. depicting daily melatonin values with cortisol levels and core body temperature in relation to sleep time [8].

Fig. 4.2 depicts two examples of limit cycles that have not been rescued. One does not have enough hours of sleep prior to H_2max and the other does not have enough sleep time after $Cmin$.

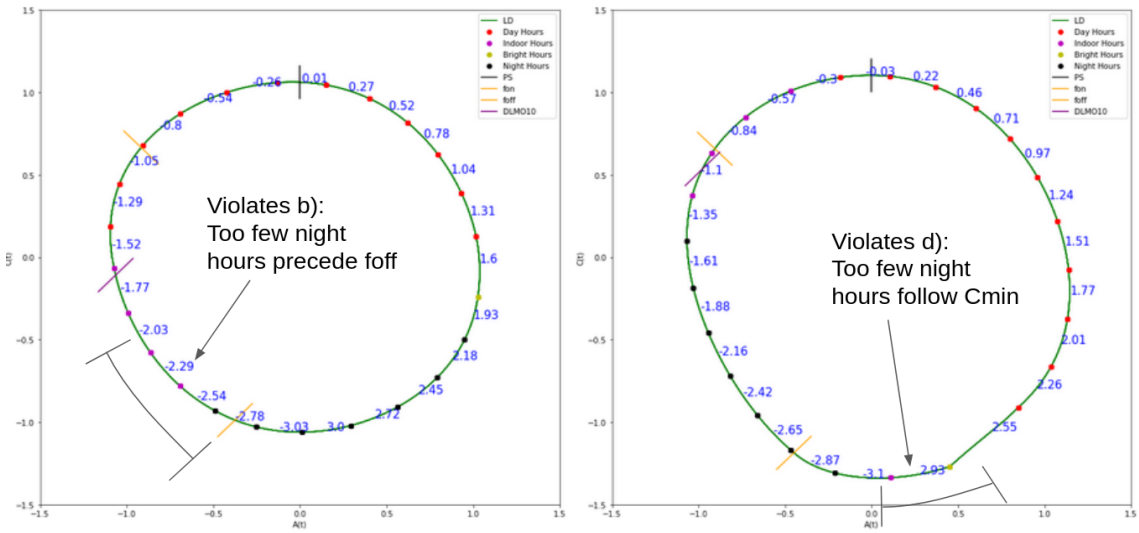

Figure 4.2 Not Rescued. Depicts examples of entrained limit cycles that do not meet the criteria for rescued. The left limit cycle does not meet the criteria for b) whereas the right does not meet the criteria for d). Note that H_2max can only come after $Cmin$ if $Cmin$ occurs shortly after lights-on and H_2max occurs during Night Hours due to the redefined values of fon/foff thus violating condition d). The previous values of fon/foff allowed for H_2max to come after $Cmin$ during Night Hours. The time condition of c) as only met for the previous values if lights-on occurred before foff which violated conditions b) and d).

Using this new concept, we explore the effects of changing the time of bright light administration on different parameter combinations. The results vary from the expected to the surprising.

4.2 Cases

Table 4.1 Bright Light Cases: Melatonin Values

Healthy w/out BL									
τ_C	p	$Mmax$	No BL	BL hr1	BL hr2	BL hr3	BL hr4	BL hr5	BL hr6
24.2	0.5	0.9	266	250	260	264	265	265	265
24.2	1.2	0	242	-	-	-	-	-	-
Non-entrained w/out BL									
τ_C	p	$Mmax$	No BL	BL hr1	BL hr2	BL hr3	BL hr4	BL hr5	BL hr6
24.4	1.7	0	-	-	232	249	259	264	267
24.4	1.7	0.1	-	-	238	257	265	271	-
24.3	2	1	-	257	-	-	-	-	-
24.7	2	1	-	-	-	-	-	-	-
No rescue w/out BL									
τ_C	p	$Mmax$	No BL	BL hr1	BL hr2	BL hr3	BL hr4	BL hr5	BL hr6
24.3	1.2	0.8	-	220	249	263	270	-	-
24.3	1.2	1	-	228	261	272	-	-	-
24.6	0.2	0.9	-	-	-	-	-	-	-

Depiction of each case considered highlighting rescued cases by showing maximum values of H_2 (melatonin concentration in blood). Hyphens indicate that the case for that hour of Bright Light (BL) either does not rescue or does not entrain. We specify the parameters for each case in the left three columns. The case without BL is represented as 'No BL' and BL administered at successive early hours make up the remaining columns. Cases are sorted by the status of the limit cycle without bright light. There are two cases of Healthy limit cycles with very different outcomes. There are four cases of non-entrained limit cycles and three cases of limit cycles that need rescuing but do entrain. Note that the role that max melatonin plays in these cases is not entirely clear other than the fact that they should be above 200 and less than 280. Less than 200 indicates the limit cycle violates condition b). Anything more than 280 indicates the limit cycle violates condition d).

In this section, we consider 9 combinations of parameters and administer bright light in the first six hours after lights-on and analyze the results. Table 4.1 depicts the different cases we consider and shows the blood melatonin concentration (in pmol/L) if the parameter combination and hour or bright light administration meet the requirements for rescued. We consider the cases by the order in which they appear in the table. Each case is accompanied by a figure which shows screenshots of the limit cycles in question.

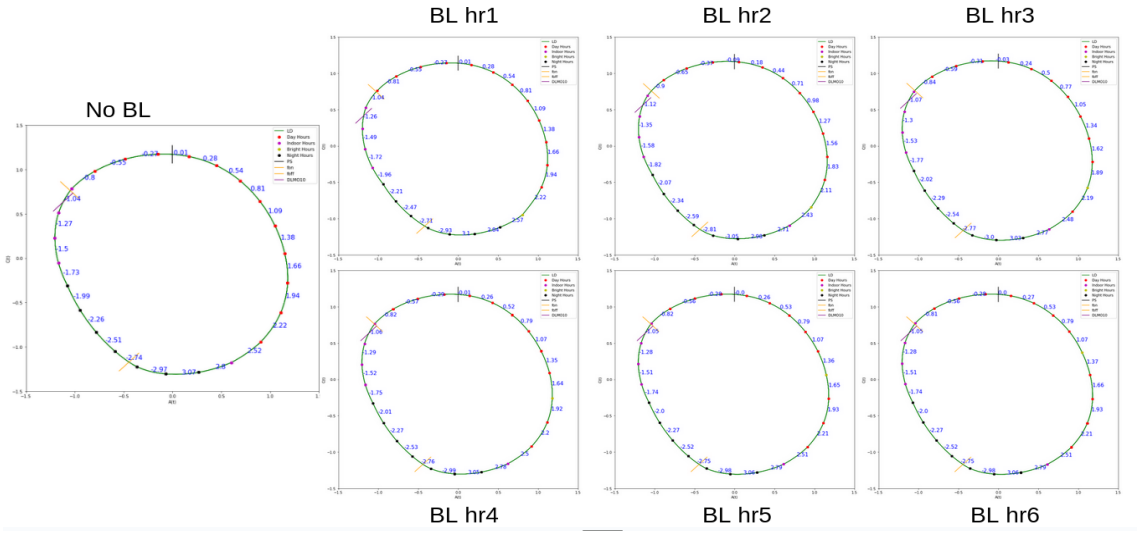

Figure 4.3 Best Healthy Case. Limit cycle is healthy after administration of bright light at any hour considered. In addition to meeting the criteria for healthy, the limit cycle without bright light exhibits a potentially beneficial quality of having fon just after Indoor Hours in anticipation of Night Hours. This allows blood melatonin to reach a max higher than it would for the case when it occurs any earlier while still meeting the criteria for sleep time after $Cmin$. Note however that the model can not predict any significant difference if fon occurs during Day Hours.

We highlight the interesting cases here. Observe in the 'Healthy w/out BL' section that it is possible to start with a limit cycle that meets the conditions and after BL fail to meet the conditions (such as in Fig. 4.4). The third non-entrained case is only rescued with bright light administered at hour 1 (Fig. 4.7). The final case (Fig. 4.11) starts with a limit cycle that just barely does not meet the criteria

for healthy. Administration of bright light changes the limit cycle only slightly in the first hour and afterwards the results are the same as the original.

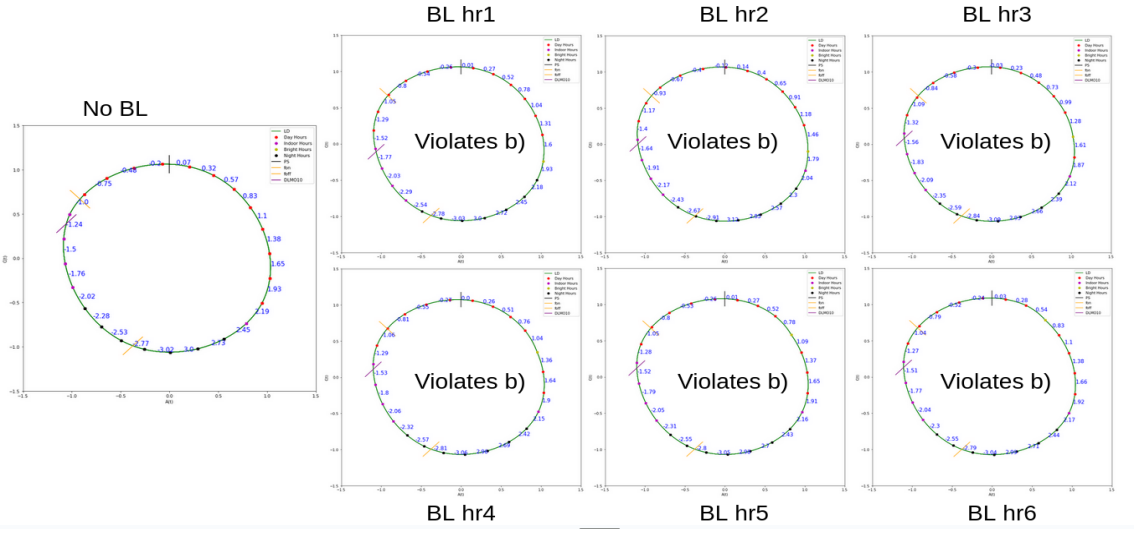

Figure 4.4 Less Desirable Healthy Case. The limit cycle is healthy without bright light, but administration of bright light yields a limit cycle that violates condition b) of rescued. Furthermore, there is not a lot of progress towards being rescued as the hour of bright light administration increases as there. Observe that the healthy limit cycle only just meets the criteria for b) (more than 2 hours of Night Hours prior to foff). Administering bright light in the first hour reduced the amount of Night Hours before foff by 2 hours and later hours does little to recover the lost time, reaching a max of 1.5 hours before foff at BL hr 4 where it stays for BL hrs 5 and 6. This case is perplexing, but it reveals that BL in part functions fundamentally as a mechanism of adjusting the phase of the limit cycle which may be interesting to consider more in-depth.

The remaining cases are interesting when taken together in that they paint a picture that shows that there's great variety in the results of bright light therapy. Also, that closely related limit cycles such as the first two non-entrained cases have subtly different results. That is, the first (Fig. 4.5) is rescued with bright light administered from hours 2 to 6 whereas the second (Fig. 4.6) is rescued only from hours 2 to 5.

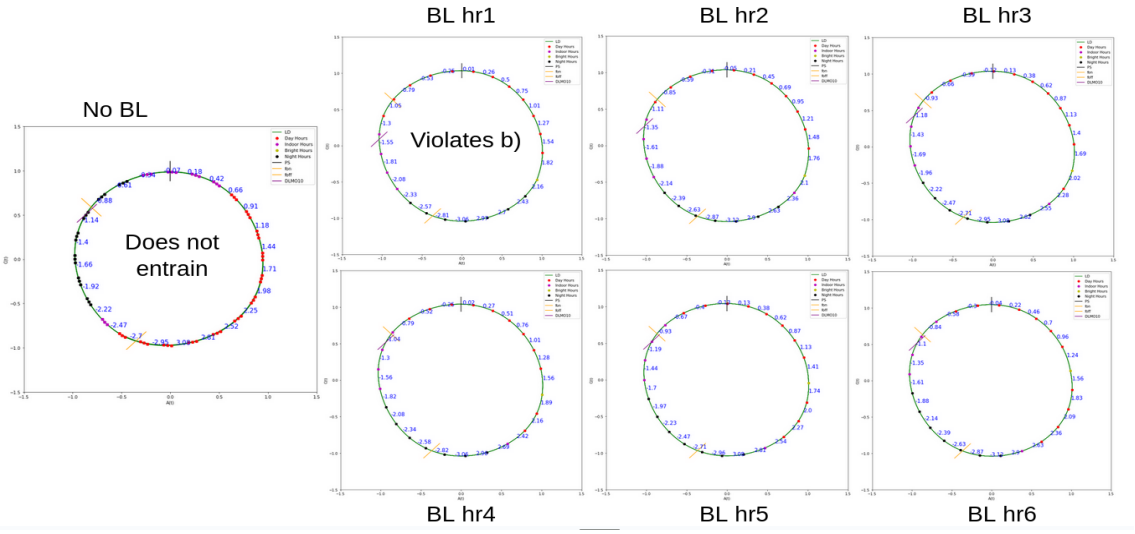

Figure 4.5 Non Entrained Case 1. Observe that every hour of bright light yields entrainment. However, bright light administered in the first hour does not rescue the limit cycle due to the fact that there are not enough Night Hours before foff. All other hours rescue the limit cycle.

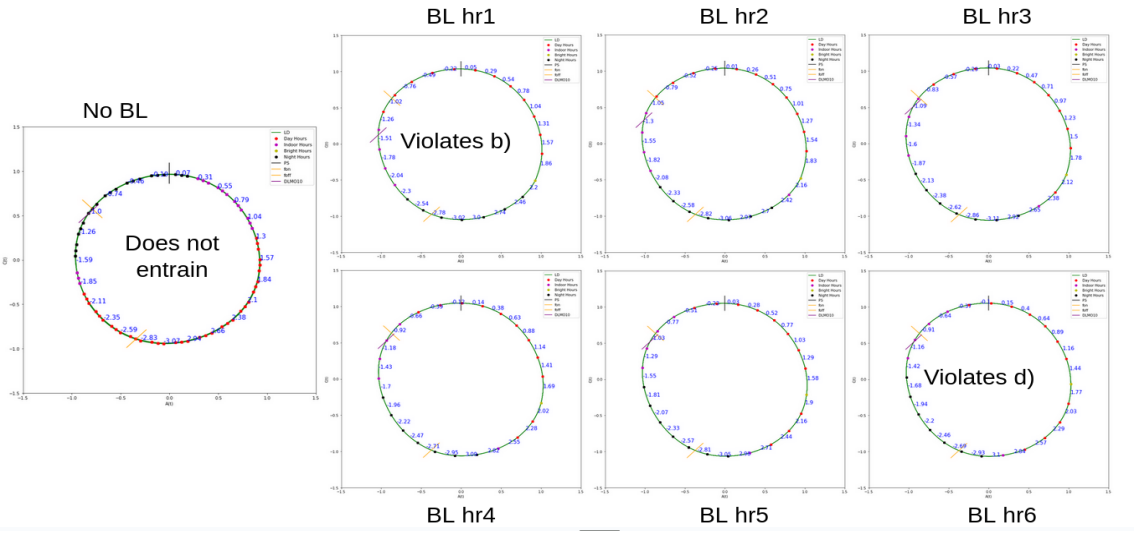

Figure 4.6 Non Entrained Case 2. Observe that every hour of bright light yields entrainment. However, bright light administered in the first and sixth hours does not rescue the limit cycle. In the first hour, it is due to the fact that there are not enough Night Hours before foff. In the sixth hour it is due to the fact that there is not enough sleep time after $Cmin$. The other hours rescue the limit cycle.

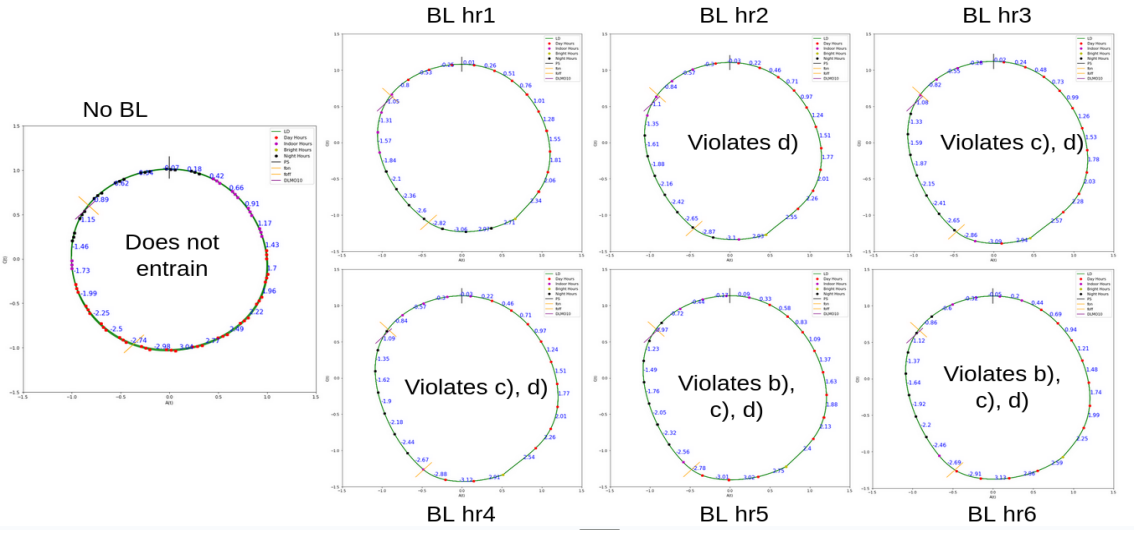

Figure 4.7 Non Entrained Case 3. Observe that every hour of bright light yields entrainment. However, only bright light administered in the first hour rescues the limit cycle. The other hours fail to rescue for different combinations of reasons. It is noteworthy that there is one specific hour of bright light administration that rescues the limit cycle.

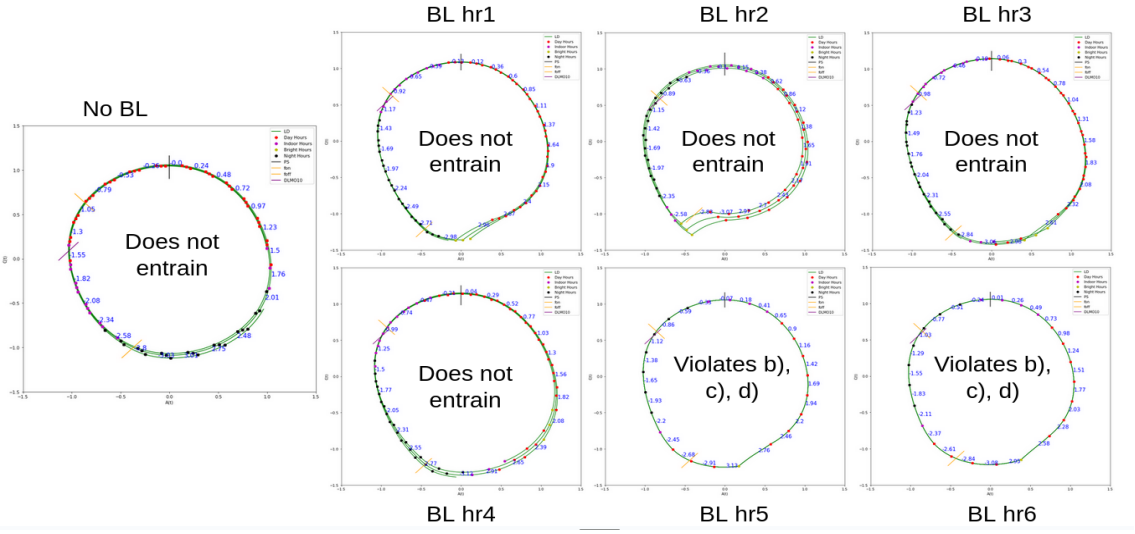

Figure 4.8 Non Entrained Case 4. Observe that only the final two hours of bright light yield entrainment. Unfortunately, they do not result in rescued limit cycles. The fact that the Night Hours are situated in the top left of the limit cycle explains why all three of the conditions are violated.

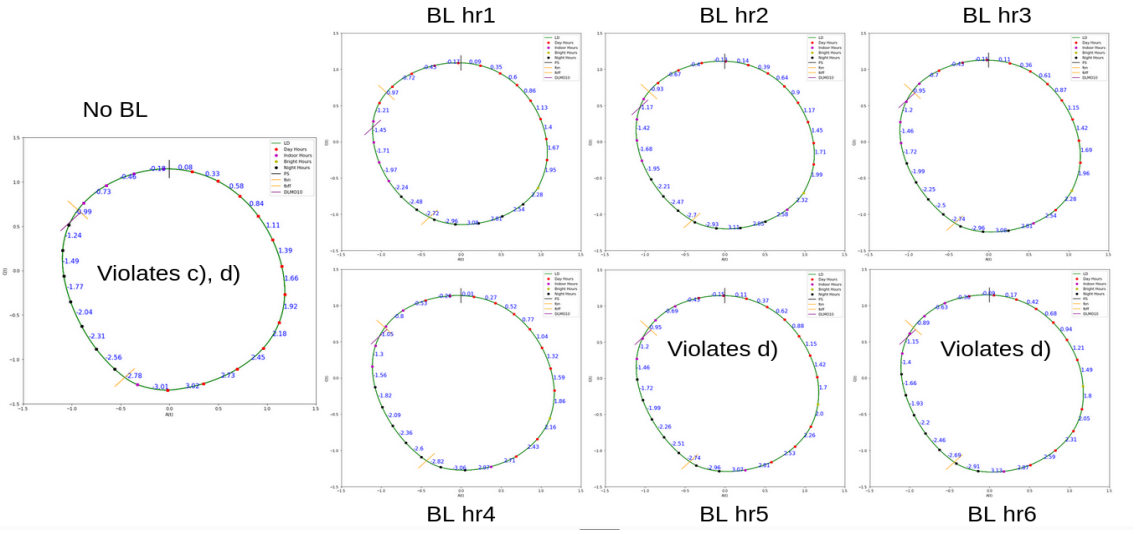

Figure 4.9 Needs Rescuing Case 1. The original limit cycle has an H_2max occurring during night hours and the time from H_2max to $Cmin$ is approximately what it should be. However, lights-on occurs before $Cmin$ meaning that both c) and d) are violated. On the other hand, bright light rescues the limit cycle when administered from hours 1 to 4 but there is not enough time between $Cmin$ and lights on for bright light administered at hours 5 and 6.

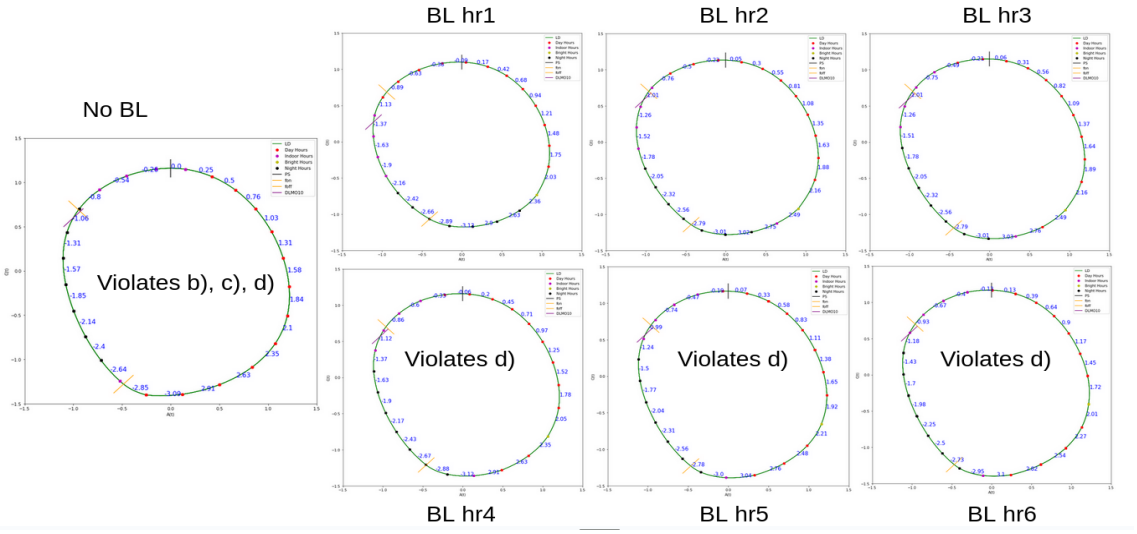

Figure 4.10 Needs Rescuing Case 2. The original limit entrains, but does not meet any of the criteria for healthy because H_2max and $Cmin$ occur just after lights-on. Bright light rescues the limit cycle when administered from hours 1 to 3 but there is not enough time between $Cmin$ and lights on for bright light administered at hours 4 to 6.

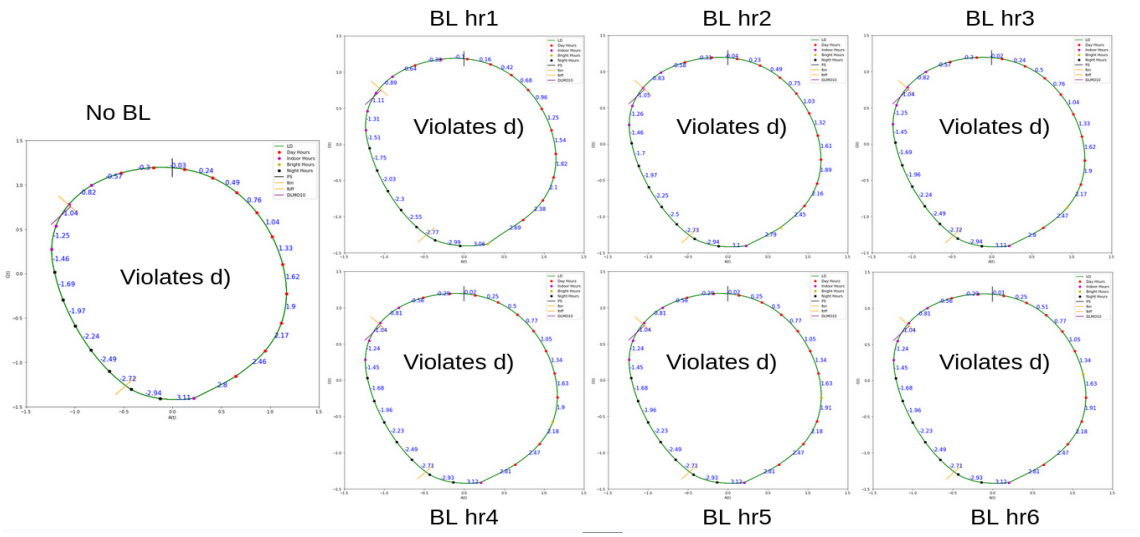

Figure 4.11 Needs Rescuing Case 3. A curious case. The original limit cycle fails to be healthy due to a lack of time between $Cmin$ and lights-on. Administering bright light at hour 1 appears to increase the difference, but still does not meet the criteria. Moving on to hour 2 the difference is the same as the original limit cycle an the results of all bright light hours after that. It would be interesting to investigate what series of factors have to be in place for no change to take place like this.

We considered 528 combinations of τ_C, p, and $Mmax$. It is difficult to represent the totality of the results by 9 cases, but they do depict the extremes and hints at the general behaviors as parameters change incrementally. We established a rather large spreadsheet in the same style as Table 4.1 should that be of interest. Essentially it says that, despite how it seemed from Chapter 3 where bright light administered at hour 5 for a long tau is the best bet (it entrains the most) the truth is that one should be deliberate about the time of bright light, tailoring it to the patient. Even when the results of bright light are similar, the resulting max melatonin values change from subtly to significantly. While it's unclear what role the specific value of max melatonin plays based on this model, it may be quite significant. In that case, the time of bright light administration is even more important.

4.3 Conclusion and Future Research

In general, bright light plays a significant role in entraining and rescuing limit cycles. We have shown that different hours of bright light administration yields entrainment for different numbers of combinations of the parameters considered here. Furthermore, different hours of bright light administration yields different *qualities* of entrainment (i.e. rescued or not and max melatonin concentrations).

With our current model, we are unable to simulate depression as we would have liked, but it is possible that with some tweaks the model can be that much closer to providing concrete answers for patients with depression or other mood disorders. The issue appears to be that light sensitivity does not effect melatonin concentration.

As such, a natural next step for the model would be to implement light sensitivity into the melatonin system. Presumably this would mean adopting the light sensitivity mechanism of the FJK model to the Unified Model's light detection mechanism in equation 2.4. We suspect that the implementation would yield the melatonin profile difference we see between healthy and depressed individuals in the cited paper [3].

Additionally, the light profile considered here appears to be that of a light-starved couch potato. An interesting approach would be to take some readings across several days and get different profiles for different weather and living conditions and explore the models simulations under those different conditions.

Likewise, research into physiologically viable parameter values for the three parameters varied here (τ_C, p, and $Mmax$) would be interesting. Is it unrealistic to expect a person's intrinsic period to be greater than 25 hours? Less than 23? Also, is it reasonable to assume that the concentration of melatonin to provide *negative* feedback on the pacemaker? What about positive feedback (which would simply mean considering negative values of $Mmax$)?

Next, since we found that the limit cycle for $\tau_C = 24.7$, $p = 2$, and $Mmax = 1$ entrains in Chapter 4, whereas the heat maps from Chapter 3 show that the same combination of parameters do not result in an entrained limit cycle, it appears that the values of ϕ_{on}/ϕ_{foff} affect entrainment, as well. Therefore, implementing another differential equation into the model that controls ϕ_{on}/ϕ_{foff} might be worth exploring. It is not clear how difficult such an implementation would be. A good start would be to see how authors of the cited article dealt with the issue [14]. It seems that they were concerned with determining such positions based on data as opposed to modeling the behavior but it is possible that some of the authors of the paper have done work that might contribute to a differential equation.

Our model simulates sleep as hours during which light input is 0 lux. It would be interesting – and more realistic – to implement an existing sleep model into our model to see what dynamics that adds. This is motivated by the extensive flow chart in the Unified Model article (their Fig. 1 on page 3) [1]. Furthermore, our own experience suggests that levels of wakefulness impact one's sensitivity to light. Does such a visceral experience translate to sensitivity as we have conceived of it in this model? Could it be associated with levels of melatonin (translating to a light sensitivity scaling with melatonin concentrations)? Does the experience translate at all to a biological effect for which we need to account in order to draw valid conclusions?

Also, testing the model with real-world data. All of the component models were tested with real world data, but we have made changes and combined parts of the models, so we can say nothing with confidence that would apply to a real-world case.

Lastly, it might be interesting to consider the necessary assumptions for the entrainment map to be valid for a general case. It seems that we need the system to be oscillatory, but would the math work for a damped oscillator? These questions require further research.

REFERENCES

[1] Romesh G. Abeysuriya, Steven W. Lockley, Peter A. Robinson, and Svetlana Postnova. A unified model of melatonin, 6-sulfatoxymelatonin, and sleep dynamics. *Journal of Pineal Research*, 2018(64), 2018.

[2] Emily R. Breslow, Andrew J.K. Phillips, Jean M. Huang, Melissa A. St Hilaire, and Elizabeth B. Klerman. A mathematical model of the circadian phase-shifting effects of exogenous melatonin. *Journal of Biological Rhythms*, 28(1):79–89, 2013.

[3] Wolnei Caumo, Maria Paz Hidalgo, Andressa Souza, Iraci L.S. Torres, and Luciana C. Antunes. Melatonin is a biomarker of circadian dysregulation and is correlated with major depression and fibromyalgia symptom severity. *Journal of Pain Research*, 2019(12):545–556, 2019.

[4] Casey O. Diekman and Amitabha Bose. Entrainment maps: A new tool for understanding properties of circadian oscillator models. *Journal of Biological Rhythms*, 31(6):598–616, 2016.

[5] Casey O. Diekman and Amitabha Bose. Reentrainment of the circadian pacemaker during jet lag: East-west asymmetry and the effects of north-south travel. *Journal of Theoretical Biology*, 437(261):261–285, 2018.

[6] Casey O. Diekman and Amitabha Bose. Beyond the limits of circadian entrainment: Non-24-h sleep-wake disorder, shift work, and social jet lag. *Journal of Theoretical Biology*, 545(111148):111148–111161, 2022.

[7] Daniel B. Forger, Megan E. Jewett, and Richard E. Kronauer. A simpler model of the human circadian pacemaker. *JOURNAL OF BIOLOGICAL RHYTHMS*, 14(6):533–537, 1999.

[8] Ian B. Hickie, Sharon L. Naismith, Rebecca Robillard, Elizabeth M. Scott, and Daniel F. Hermens. Manipulating the sleep-wake cycle and circadian rhythms to improve clinical management of major depression. *BMC Medicine*, 11(79):1–27, 2013.

[9] Daniel F. Kripke. Light treatment for nonseasonal depression: speed, efficacy, and combined treatment. *Journal of Affective Disorders*, 49(2):109–117, 1998.

[10] Richard E. Kronauer, Daniel B. Forger, and Megan E. Jewett. Quantifying human circadian pacemaker response to brief, extended, and repeated light stimuli over the photopic range. *JOURNAL OF BIOLOGICAL RHYTHMS*, 14(6):501–515, 1999.

[11] Jorge Mendoza and Guillaume Vanotti. Circadian neurogenetics of mood disorders. *Cell and Tissue Research*, 2019(377):81–94, 2019.

[12] Jonatan Pena Ramirez, Luis Alberto Olvera, Henk Nijmeijer, and Joaquin Alvarez. The sympathy of two pendulum clocks: beyond huygens' observations. *Scientific Reports*, 6(23580):898–902, 2016.

[13] Ueli Schibler and Paolo Sassone-Corsi. A web of circadian pacemakers. *Cell*, 111(7):130, 2002.

[14] Melissa A. St Hilaire, Claude Gronfier, Jamie M. Zeitzer, and Klerman Elizabeth B. A physiologically based mathematical model of melatonin including ocular light suppression and interactions with the circadian pacemaker. *Journal of Pineal Research*, 2007(43):294–304, 2007.

[15] Steven H. Strogatz. *Nonlinear Dynamics and Chaos: With Applications to Physics, Biology, Chemistry, and Engineering, 2nd Ed.* CRC Press, 2015.

[16] Anna Wirz-Justice. Beginning to see the light. *ARCH GEN PSYCHIATRY*, 55(10):861–862, 1998.